Marine Geology 264 (2009) 28–40

Contents lists available at ScienceDirect

Marine Geology

journal homepage: www.elsevier.com/locate/margeo

Geomorphology, stability and mobility of the Currituck slide

Jacques Locat [a,*], Homa Lee [b], Uri S. ten Brink [c], David Twichell [c], Eric Geist [b], Mylène Sansoucy [a]

[a] Department of Geology and Geological Engineering, Université Laval, Québec, Qc, Canada
[b] United States Geological Survey, Menlo Park, CA, United States of America
[c] United States Geological Survey, Woods Hole, MA. United States of America

ARTICLE INFO

Article history:
Accepted 15 December 2008

Keywords:
Currituck
submarine slides
mobility
stability
yield strength
flow

ABSTRACT

Over the last 100,000 years, the U.S. Atlantic continental margin has experienced various types of mass movements some of which are believed to have taken place at times of low sea level. At one of these times of low sea level a significant trigger caused a major submarine mass movement off the coast of Virginia: the Currituck slide which is believed to have taken place between 24 and 50 ka ago. This slide removed a total volume of about 165 km^3 from this section of the continental slope. The departure zone still shows a very clean surface that dips at 4° and is only covered by a thin veneer of postglacial sediment. Multibeam bathymetric and seismic survey data suggest that this slide took place along three failures surfaces. The morphology of the source area suggests that the sediments were already at least normally consolidated at the time of failure. The slide debris covers an area as much as 55 km wide that extends 180 km from the estimated toe of the original slope. The back analysis of slide initiation indicates that very high pore pressure, a strong earthquake, or both had to be generated to trigger slides on such a low failure plane angle. The shape of the failure plane, the fact that the surface is almost clear of any debris, and the mobility analysis, all support the argument that the slides took place nearly simultaneously. Potential causes for the generation of high pore pressures could be seepage forces from coastal aquifers, delta construction and related pore pressure generation due to the local sediment loading, gas hydrates, and earthquakes. This slide, and its origin, is a spectacular example of the potential threat that submarine mass movements can pose to the US Atlantic coast and underline the need to further assess the potential for the generation of such large slides, like the Grand Banks 1927 landslide of similar volume.

© 2008 Elsevier B.V. All rights reserved.

1. Introduction

Experience with tsunamis (e.g. Tinti, 1993) has shown that they can be caused by either movements along offshore faults (tectonic tsunamis) or by large submarine landslides (landslide tsunamis). The magnitude of landslide-generated tsunamis depends strongly upon the size of the slide and how the landslide moves as it fails and flows. Submarine mass movements along the U.S. Atlantic continental margin have been recognized for many years (e.g. Booth et al., 1993; Twichell et al., 2009-this volume) but it is only recently that their potential tsunamigenic contribution has been considered (ten Brink et al., 2007). As is presented elsewhere, major mass movements that have taken place on the Atlantic continental margin over the last 100,000 years (Lee, 2009-this volume) may be good candidates for tsunamigenic mass movements. Many of these slides have left a clear signature which enables a minimum definition of the initial stratigraphic and physical conditions prior to failure, and also of the volume and shape of their deposits. One of them, the Currituck slide (Fig. 1) has been selected to evaluate the tsunamigenic potential of such slides. The Currituck slide has been selected to be analyzed as part of a USGS effort sponsored by the Nuclear Regulatory Commission to perform an evaluation of the risk of damaging tsunamis impacting the US East coast (ten Brink et al., 2007). This paper is part of an overall effort to consider various geoscientific aspects of tsunamigenic mass movements using the Currituck slide (Fig. 1), as a methodological example in a way similar to what has been done for the Palos Verdes slide off Los Angeles (Locat et al., 2004). It also provides an opportunity to discuss the potential triggering mechanisms and mobility of these very large submarine mass movements.

The Currituck slide (Fig. 1), located northeast of Cape Hatteras, has been investigated earlier by Bunn and McGregor (1980) and Prior et al. (1986). Prior et al. (1986) presented a detailed description of the stratigraphy and morphology of the slide source area based on sidescan sonar imaging and high resolution seismic surveys. From a morphological viewpoint, the model (Fig. 1c and d) proposed by Prior et al. (1986) does agree very well with what is observed from the multibeam bathymetry image obtained more recently (Fig. 1b). They concluded that two slides could be observed (Fig. 1d) having a total volume of 128 km^3. According to Prior et al. (1986) the sliding took

* Corresponding author. Tel.: +1 418 656 2179; fax: +1 418 656 7339.
E-mail address: jacques.locat@ggl.ulaval.ca (J. Locat).

0025-3227/$ – see front matter © 2008 Elsevier B.V. All rights reserved.
doi:10.1016/j.margeo.2008.12.005

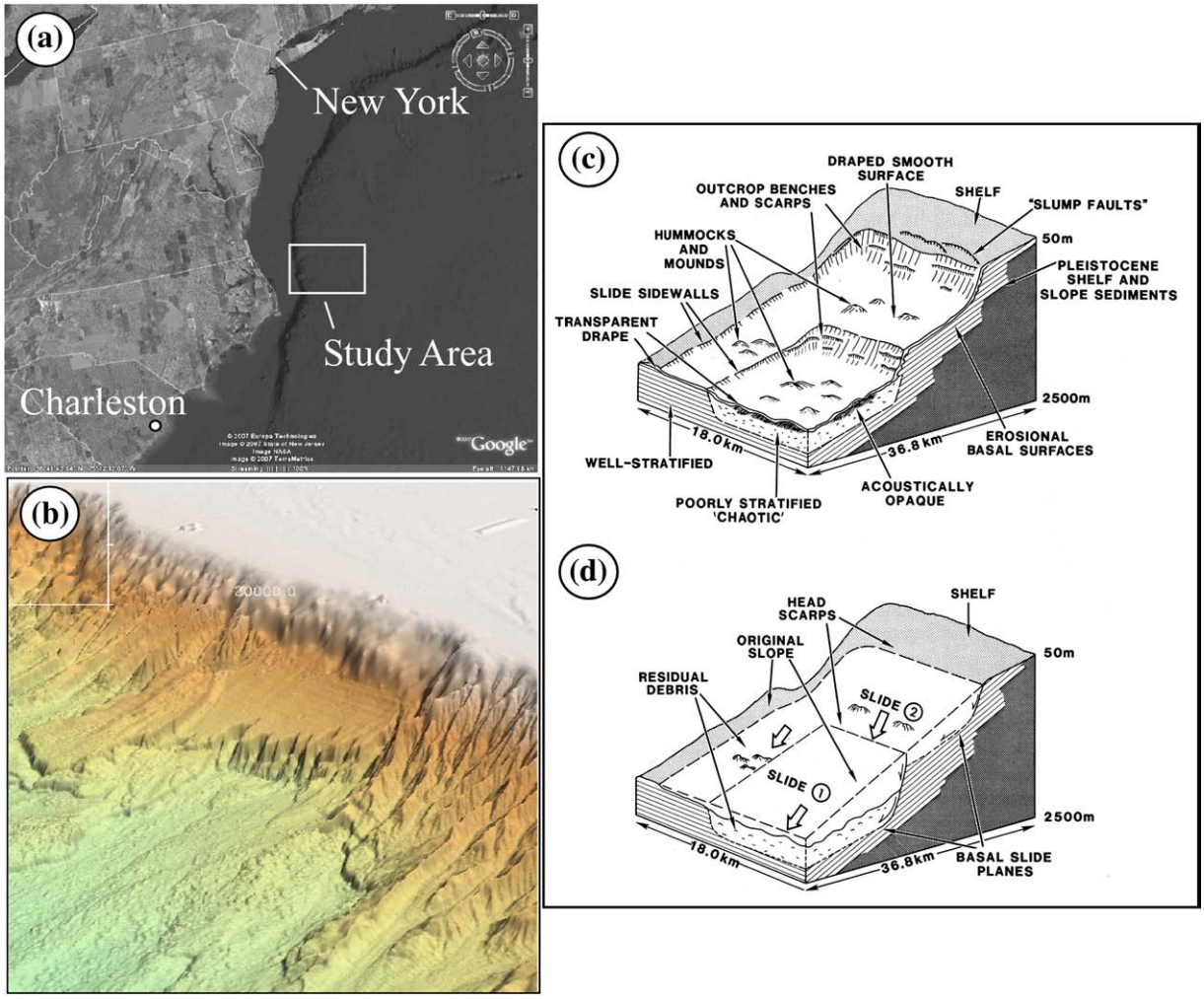

Fig. 1. Location of the Currituck Slide., (a): study area, (b) the Currituck slide looking towards the south west, (c) and (d): schematic views of the Currituck slide taken from Prior et al. (1986).

place largely in gently seaward dipping Pleistocene sediments. They concluded, based on sedimentation rate estimates, that the slides occurred 43,300 to 22,500 years BP. They also proposed that the instability could be the result of the progradation of a delta over the shelf edge but, because the failure surface is clean of deltaic sediments, they conclude that it must have taken place towards the end of the period of rapid sedimentation. Lee (2009-this volume), after reviewing the available data also concluded that the Currituck slide likely took place between 25 and 50 ka.

For tsunami initiation, a key question here is, whether or not, the slides identified by Prior et al. (1986) represent different events or if they were created as part of a single event. It will be shown that the mobility analysis presented below suggests that they must have been a single event.

The objectives of this research effort is to carry out a slope stability and mobility analysis of the Currituck slide (Fig. 1) based on previously acquired information in order to provide input data into a tsunami analysis of the Currituck slide (Geist and Parsons, 2009-this volume). To achieve this objective there is a need to establish the following conceptual models,: (1) a morpho-stratigraphic model of the departure zone of the slide area, and (2) a depositional model in the run-out zone which are based on engineering judgment, existing geophysical data and limited sediment core data (Twichell et al., 2009-this volume).

These conceptual models are used as input to analyze the stability of the initial slope using SlopeW (Krahn, 2004) and the mobility of the failed mass using BING (Imran et al., 2001b). The approach used to gather the information for these models is presented below.

2. Approach

The approach used follows most of the steps proposed by Locat et al. (2004), which includes: (1) morphological analysis, (2) estimation of geotechnical properties of the soil or rock for limit equilibrium analysis of slope failure conditions, (3) and post-failure flow dynamics (analysis of the run-out characteristics of the failed mass). At the end of this analysis we provide conclusions on:

1. The geometry of the source area prior to failure.
2. The potential triggering mechanisms and potential failure scenarios.
3. An estimate of the volume of failed material and run-out characteristics of the slide.
4. Inferences on initial velocity and acceleration of the failed mass obtained from the mobility analysis.

The geomorphological analysis makes use of seismic and multi-beam data sets (Twichell et al., 2009-this volume; Chaytor et al., 2007, 2009-this volume) and also of the stratigraphic interpretation provided by Prior et al. (1986). Since no direct geotechnical data are available for the sediments in the Currituck slide area, we derived the

strength parameters from the limited lithological data available from Prior et al. (1986, describe below) and from local slope morphological characteristics. The stability back analysis was conducted using the observed failure plane geometry.

The limit equilibrium state of the slope is assumed under ambient and seismic loading and for various conditions of pore pressure. It is assumed here that the material failure behavior follows a Mohr-Coulomb failure criterion such as:

$$\tau^* = c' + (\sigma - u)\tan\phi', \tag{1}$$

where τ^* is the shear strength of material that can be mobilized along the failure plane, c' the cohesion, σ the total stress, u the pore pressure and φ' the friction angle. The computation was carried out using the General Limit Equilibrium (GLE) method (Krahn, 2004). The role of pore pressure was evaluated using the pore pressure ratio (r_u) calculated using the buoyant unit weight of the sediments (γ^*):

$$r_u = \frac{u}{\gamma^* h}, \tag{2}$$

where h is the thickness of the material above the potential failure plane. For a r_u value of 1, the pore pressure is equal to the weight of the sediments.

Using the GLE method, the effects of earthquakes are taken into account by the coefficient of seismic acceleration k:

$$k = \frac{\alpha W}{g}, \tag{3}$$

where α represents the pseudostatic acceleration and g the gravitational acceleration, and W the total weight of the sediment, k can be seen as a percentage of g.

For post-failure analysis of the failed mass, we used a 1D-flow dynamics model, BING, presented by Imran et al. (2001b), which has been developed for the study of debris flows. BING can be used with various rheological models: Bingham, Herschel-Bulkley and Bilinear. In our analysis, we use both bilinear and Bingham flow models. The Bilinear model was proposed by Locat (1997) to describe the rheology of clayey silt or silt mixtures, which often present a pseudo-plastic behavior. A similar proposal was made by O'Brien and Julien (1988) also for sediments with high silt content. The Bilinear model assumes that the initial phase of the flow is Newtonian (Fig. 4 in Locat et al., 2004) and evolves, after reaching a threshold shear rate value (γ_o), into a Bingham type flow. The constitutive equation proposed by Locat (1997) for Bilinear flow is expressed by:

$$\tau = \tau_{ya} + \mu_{dh}\gamma - \frac{\tau_{ya}\gamma_o}{\gamma + \gamma_o}, \tag{4}$$

where τ is the flow resistance, τ_{ya} the yield strength, μ_{dh} the plastic viscosity, γ the shear rate, and γ_o the shear strain rate at the transition from a Newtonian to a Bingham behavior.

In BING (Imran et al., 2001b), Eq. (4) is re-written

$$\frac{\tau}{\tau_{ya}} = 1 + \frac{\gamma}{\gamma_r} - \frac{1}{1 + r\frac{\gamma}{\gamma_r}}, \tag{5}$$

where γ_r, is the strain rate defined as

$$\gamma_r = \frac{\tau_{ya}}{\mu_{dh}} \tag{6}$$

and r the ratio of the strain rates,

$$r = \frac{\gamma_r}{\gamma_o}. \tag{7}$$

The Herschel Bulkley model corresponds to the following expression:

$$\tau = \tau_y + K\gamma^n \tag{8}$$

where

$$K = \frac{\tau_y}{\gamma_r^n} \tag{9}$$

and is equivalent to a Bingham model when the exponent 'n' equals 1. For the mobility analysis both Bingham and Bilinear models are used.

For the Currituck slide, no rheological data are available. Consequently, we rely on the morphology of the depositional area to help estimate the yield strength. This is done using the following equation initially proposed by Johnson (1970):

$$\tau_{ya} = H_c\gamma^* \sin\beta, \tag{10}$$

where H_c is the critical thickness (in meters) of the debris flow deposit, γ^* is the buoyant unit weight (in kN/m^3) of the debris flow material and β the angle (in degrees) of the slope over which the debris flow came to rest.

The values related to the plastic viscosity, *i.e.* the strain rate, γ_r, and the ratio of strain rates, r, will be estimated from a parametric analysis to find the best values which can fit the observed geometric characteristics in the run-out zone, the travel distance in particular. The value of γ_r can also be estimated from rheological testing result which have shown that the value of γ_r is about 1000 for clays (Locat, 1997; Locat and Lee, 2002; Lee et al., 2007) but can be as low as 10 for sand (Jeong et al., 2007).

3. Geomorphological analysis

The pre and post slide geomorphology of the Currituck slide has been detailed by Prior et al. (1986) and is shown in Fig. 1b and c. Their inferred morphology of the slope prior to failure is shown in Fig. 1d and is based on both sidescan and seismic data. Prior et al. (1986) have shown that the failure planes observed were directly following regular layers (reflectors) observed on the seismic records (e.g. see Fig. 3 in Prior et al., 1986). They also report that, according to core observations collected by Bunn and McGregor (1980), the sliding mass would have moved over a smooth seaward-dipping horizon of dry friable clay of early Pleistocene age. Details of the morphology of the source area of the slide are shown in Figs. 1b and 2, which show images and profiles generated from the multibeam data that was collected subsequent to the study by Prior et al. (1986). The multibeam data was coupled to the available seismic data by Twichel et al. (2009-this volume) to evaluate the distribution of the debris and to provide an estimate of the volume, as it will be described below, which is around 150 km^3, i.e. of the same order of what has been estimated by Prior et al. (1986) and by the detailed analysis of the morphology of the strating zone presented hereafter.

Prior et al. (1986) noted the presence of two slides: slide 1 (lower, assumed to have started first) with an escarpment dipping at about 15–30°, and slide 2 with an escarpment (upper) of about 9 to 10° and (Fig. 2c). The actual slope morphology of the upper escarpment is similar to the adjacent areas suggesting that some sediment draping took place after the slide. The multibeam data has shown that the slope angle in the lower escarpment can reach values as high as 30°, particularly in the gullied sections (Figs. 2b and 3, see Fig. 5 in Prior et al., 1986). Prior et al. (1986) also noted, from seismic survey, that within the lower escarpment there were outcrop benches. This is also well seen from the detailed bathymetry shown in Fig. 2b for the various planar surfaces also showing the influence of bedding on the shape of the failure surface. In looking at the profile along line 2 in Fig. 2b, the control of the bedding on erosion is also seen by the position of the bottom of the small canyons (dashed line for profile 2 in Fig. 2b) that are also aligned at the same orientation as the slide 2 failure surface. Prior et al. (1986) observed from seismic surveys, that the surface below the lower escarpment was covered by debris coming from slide 2 (see also Fig. 1c and d). Below the lower

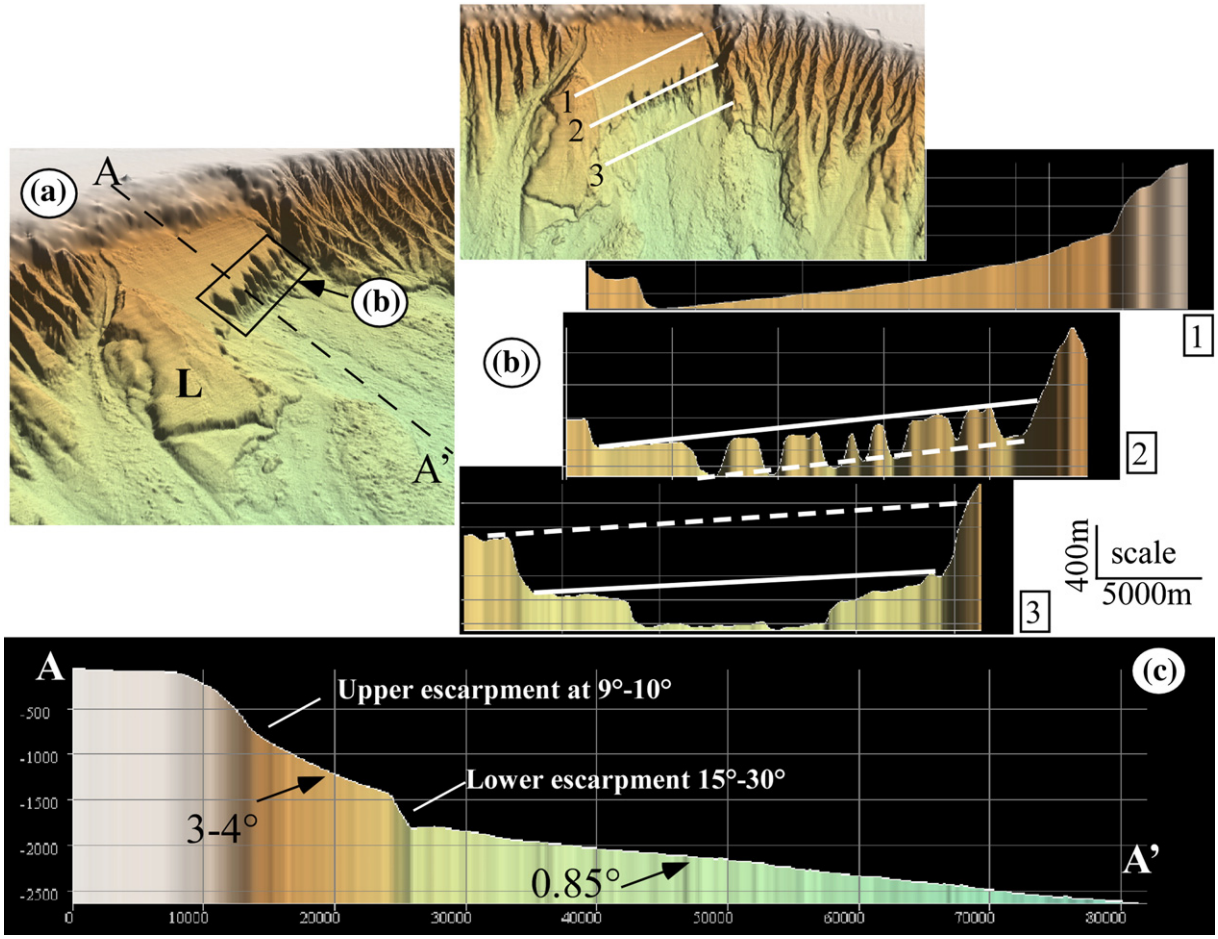

Fig. 2. Topographic profiles across the upper head of the Currituck slide showing three potential failure planes.

escarpment, the cross section shown in Fig. 2b for line 3 reveals that there is another depression which likely represents the expression of another failure surface, more restricted laterally than the other ones and buried under some debris.

The seafloor imagery around the slide area is shown in Fig. 3 showing the well developed canyon system on both sides of the slide area. South of the slide area, one lineament cuts across the canyon ridges and is believe to represent the trace of a fault line but this could not be confirmed by the seismic data of Prior et al. (1986). Another observation shown in Fig. 3 is that of an area just south of the lower escarpment which is rather smooth and gently sloping towards the south. It may represent the remnants of the extension of a low stand Pleistocene delta as postulated by Poag and Sevon (1989).

Using the pre- and post-slide morphostratigraphic models of Prior et al. (1986) and using recent multibeam sonar data, a morphostratigraphic model of the slide, prior to failure, is shown in Fig. 4. The main modification of this model, as compared to the model shown in Fig. 1d, is the addition of a delta, as suggested by Poag and Sevon (1989), but its offshore extension is not precisely known. The position of the toe of the delta has been estimated by extending the location of the delta toe that is still preserved along the southern edge of the failure across the failed area and is shown as a smooth arc (Fig. 3). The length of the center line of the failed area is taken from the upper escarpment to the proposed toe of the slide area before failure and is about 30 km away from the upper scarp.

Since a prograding delta may play a major role of the stability of a slope, its position become a significant factor. As mentioned above, the actual extent of that delta is not known nor is its shape. The foreslope of a delta can vary significantly with depth. For example, the actual foreslope of the Fraser delta may have been as high as 15° for water depth of less than 200 m but becomes less than 2° at greater water depths (Christian et al., 1997). As observed by Prior et al. (1986) the actual failure surfaces are only covered by a thin veneer of Pleistocene sediments thus suggesting that when the slide took place the actual sedimentation originating from the shelf delta was more or less stopped at the time of the slide event.

The cross-section shown in Fig. 4 was constructed considering the following elements:

1. Based on Prior et al. (1986) who suggested that the timing of the event could coincide with low sea level indicating that a delta was extending into deeper water or near the shelf. This timing is also supported by the more recent analysis of Lee (2009-this volume) and by the absence of deltaic sediments on the failure surfaces (Prior et al., 1986).
2. The topset beds of the delta (having a slope of about 1°) extended as much as much as 1 to 5 km seaward of the present shelf edge.
3. The pre-slide surface topography is assumed to be parallel to the surface of the part of the delta that is still preserved south of the failure and extended until it intersected the present sea floor, *i.e.* at about 30 km from the actual shelf edge.
4. Most of the slide took place in well bedded silt-clay sediments dipping seaward at about 3°.

From this re-construction, it appears that the maximum thickness of the mass involved in the slide is about 750 m ('h' in Fig. 4) at the base of the lower scarp (note that the actual height of the scarp is about 350 m because the upper part has been removed when slide 2 took place, see also Fig. 1d). Using the cross section shown in Fig. 4 and

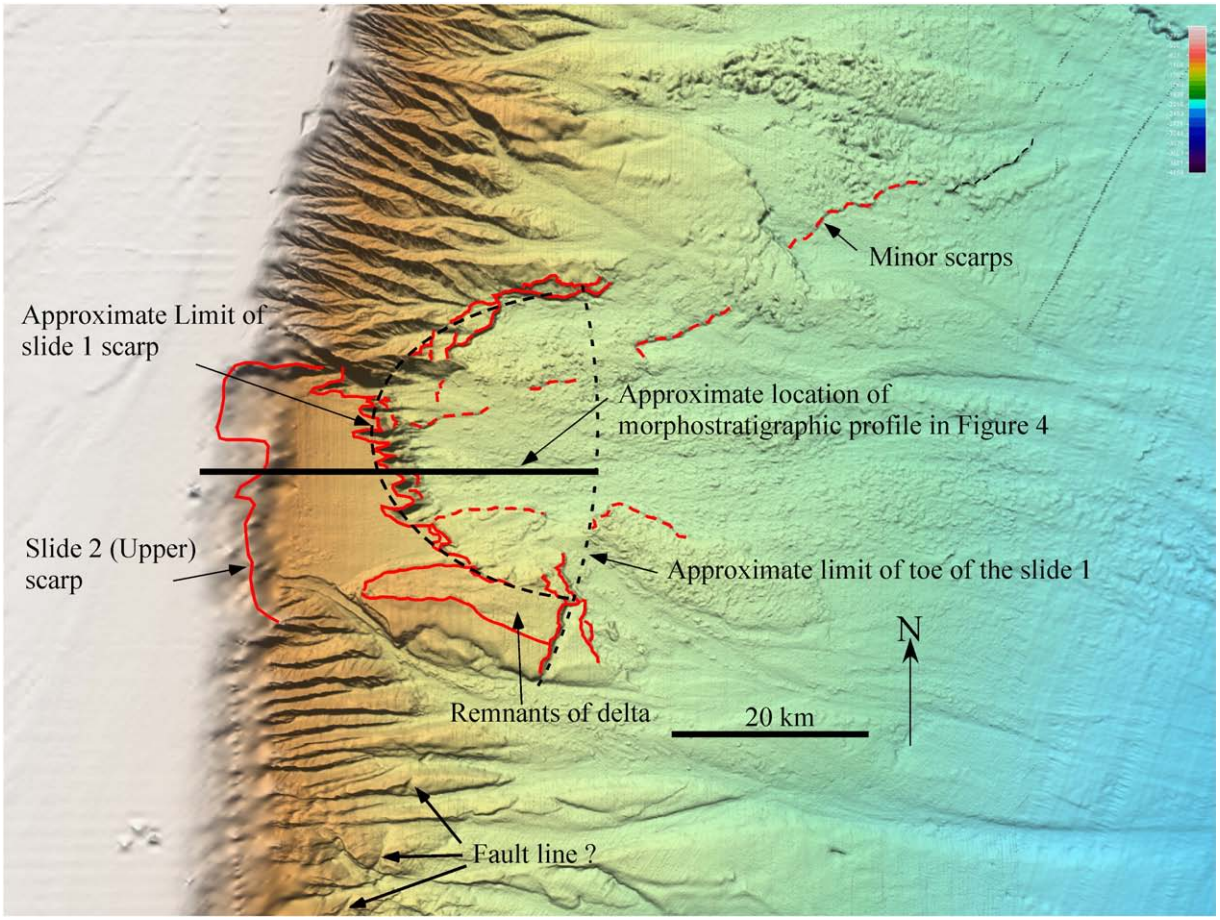

Fig. 3. Identification of the main morphological signs used for generating the morpho-stratigraphic model shown in Fig. 4.

the available bathymetry, we have estimated that the volume involved is about 165 km^3, i.e. 108 km^3 and 57 km^3 for slide 1 and 2 respectively.

When we look at the actual slide morphology (Figs. 2 and 3) and the actual slope angles, the clean surface exposed just above the lower scarp suggests that the failure developed rapidly, much like what has been modeled for the Storegga slide (Bryn et al., 2004; Kvalstad et al., 2005). The main similarity between the Storegga and the Currituck slides is the control of the bedding on the location of the failure surface.

4. Stability analysis

The approach to carry out the slope stability analysis of the Currituck slide requires a morphosedimentological model (Fig. 4) and estimates of the geotechnical properties of the sediments involved so that a geotechnical model can be established (Fig. 5). Estimation of pore pressure conditions and identification of potential triggering mechanisms such as earthquake or loading due to delta progradation (e.g. Fig. 5) must be considered. Since there are uncertainties about many of these elements, the analysis will be carried using a parametric approach, i.e. identifying the potential range of variables and using known characteristics of the slide and its deposits to constrain the interpretation of the results. For example, since we are analyzing a failure, the factor of safety is considered equal to unity. Using the known post-slide morphology of slide 1 and 2, their geometric characteristics can be used to define the failure plane, thus restricting the search for the location and shape of the failure plane to the existing ones. The estimated volume of the debris (Twichell et al., 2009-this volume) will also help constrain the geometry of the slope prior to failure.

4.1. Strength parameters

To evaluate the slope stability of the Currituck slide, geotechnical information is needed on strength parameters (e.g. Eq. (1): cohesion and friction angle). The only available information on the sediment

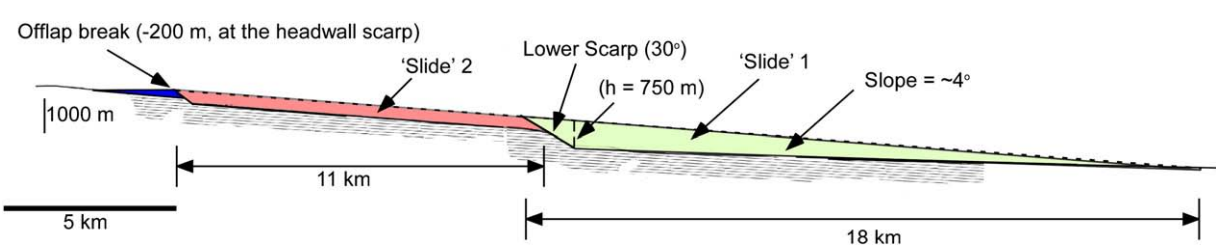

Fig. 4. Adaptation (at scale) of the model of Prior et al. (1986) based on recent bathymetry data. Note that the sub-aerial part of the delta has advanced about 2.5 km over the shelf. The model also considers a scarp slope of 30°. The surface of the delta is at -200 m.

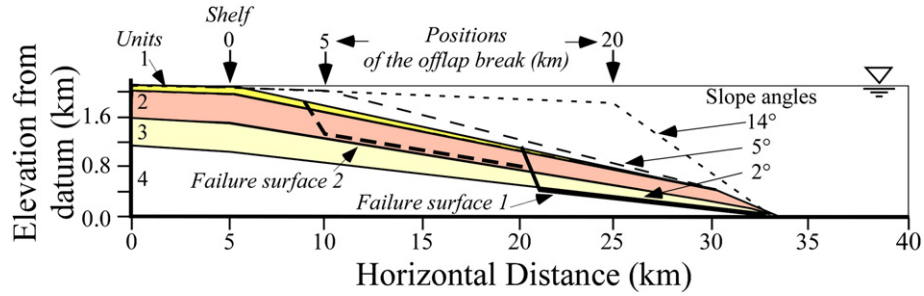

Fig. 5. Simplified model used for slope stability analysis with SLOPEW for slide 1 and 2, showing the stratigraphic units (1 to 4, see text for explanation), the failure surfaces used for slide 1 and 2, and the hypothetical deltaic infill for a delta edge located at 0, 5 and 20 km from actual shelf break position assuming a fix position of the base of the foreslope. (Vertical scale exaggeration is 3.75).

involve is that they consist mostly of a friable clay. So, in the absence of direct measurements on samples from the Currituck slide area, the strength parameters are derived from known local morphological information. For example, strength parameters can be estimated on the basis of equilibrium slope angles in a given area by assuming that the slope angle may reflect the intact strength of the sediments. This is mostly valid only for slopes which have been eroded (Locat, 2001). The slopes of the area can be grouped into three categories (Figs. 1 and 3). The first category slopes generated by sediment accumulation near the shelf edge resulting in prograding clinoforms with surface slopes varying between 4° and 10°. The second category includes slopes formed by erosional processes associated with submarine canyon development. In this case, slope angles can be as high as 30°. The third category is for slopes resulting from mass failures along failure planes that are more or less controlled by the bedding plane of sediments underlying the continental slope (Prior et al., 1986). The flat surface at the center of the Currituck slide is an excellent example (Figs. 1, 2 and 3) of the low shear strength mobilized at the time of failure. The failure surface also includes escarpments, which likely fail by extension (as part of the failure process), the lower one having slope angles similar to what is seen in the neighboring canyons. Therefore, eroded areas of the Currituck slide area do provide indications on the strength parameters, and the friction angle in particular, and for the sake of the back analysis of the slide, a friction angle value of 30° is seen adequate. Such a value is similar to what has been measured for the Hudson Apron sediments for clayey sediments (Locat et al., 2003).

A slope angle close or lower than the friction angle along canyon walls suggests that the cohesion does not contributes significantly to the long-term strength of the sediments involved. If we assume a constant cohesion with depth, its relative contribution to the shearing resistance rapidly diminishes with depth as shown in Fig. 6, when considering an infinite slope analysis. In the case computed in Fig. 6, we used a cohesion of 10 kPa and 100 kPa and, in both cases, the contribution of the cohesion to the shearing resistance (Eq. (1)) reduces to less than 10% at a depth in the sediment greater than 200 m, and for a failure surface inclined at 5°.

Fig. 5 presents a geological cross section showing four units which are chosen to reflect potential change in the sediment properties with depth, not the actual seismo-stratigraphic units of Prior et al. (1986). Buoyant unit weights of 8, 10 and 10 kN/m^3 were given for layers 1, 2, and 3 respectively. At the top, unit 1 represents deltaic sediments with properties taken with a friction angle of 30° and no cohesion. Unit 2 and 3 are believed to consist of layered clayey sediments, and unit 4 taken as impermeable bedrock. In any case, layer 4 is not directly involved in the slide since the known location of the failure place limits its position in the friable clay layer. Layers 2 and 3 were given a friction angle of 30° and 25° and a cohesion of 8 kPa (using here Hudson Apron data of Locat et al., 2003) and 100 kPa respectively. The choice of a higher cohesion for unit 3 has been done to reflect the relative increase in strength due to aging and is within values expected for soft rocks (Barton, 1976). Since the positions of the failure planes are already fixed for the back analysis, the mobilized shearing resistance is constrained to these surfaces so that the remaining instability factors are link to generation of excess pore pressures or the loading (sediment progradation). As it is the case for very low angle failure surfaces, it will be seen below that the excess pore pressure is a much more significant instability factor than the friction angle and cohesion alone.

4.2. Excess pore pressures

The significance of pore excess pore pressures can be postulated by the presence of the very low angle of the exposed failure surface which developed in sediment that was at least normally consolidated (according to canyon slope angles close to 30°). This can be explain by considering Eq. (1) where for a friction coefficient of 30°, and even using no cohesion ($c = 0$), the mobilized shear strength on a low angle slope would be very high so that only high excess pore pressures (u) could reduce the shearing resistance along such a low-angle failure plane.

High pore pressures can result from one, or a combination, of the following processes: groundwater seepage forces generated by either deltaic accumulation or a particular coastal configuration of the underlying aquifer, gas hydrates, and earthquakes. Erosion at the base of the

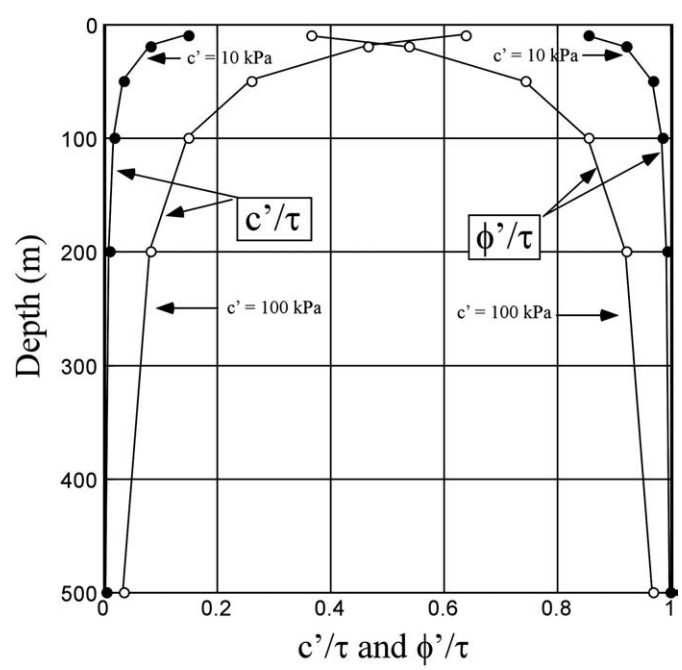

Fig. 6. Relative contribution of the cohesion and of the friction angle on the shear strength mobilized on a failure plane (Eq. (1)), considering an infinite slope approach inclined at 5° and with cohesion values of 10 kPa and 100 kPa and a friction angle of 30°.

continental slope, which is a slow process, cannot alone generate the high excess pore pressures required for failure to take place.

Excess pore pressures originating for a coastal aquifer or the formation of thick sedimentary sequences cannot be estimated for the Currituck area. The only known study of this type has been carried out by Dugan et al. (2003) and Dugan and Flemings (2005) for the continental shelf along the New Jersey continental slope (about 400 km to the North). They have modeled very high pore pressure generation near the base of the continental slope as a result of sediment consolidation. However, the slope angles in the canyons near Currituck would indicate that if such a process has been effective in the past, it is not any more. Even more, the slope angle at about 30° for the lower escarpment also suggests the excess pore pressure were not significant after the slide event. This may suggest that the required excess pore pressure for failure to take place was of limited duration.

Earthquakes are known to trigger large submarine mass movements as they both increase the gravitational forces and pore pressures (Locat and Lee, 2002). The layering observed by Prior et al. (1986) on the seismic profiles may indicate the presence of coarser (sand ?) horizons. In such a case, Kokusho and Kojima (2002) have shown that a strong earthquake could generate a water film at the interface between layers of contrasting hydraulic conductivity (e.g. clay over sand, or clay over silt) thus greatly reducing the shearing resistance at the interface between these layers.

4.3. Stability back analysis

For the following back analysis of the Currituck failure, we adapted the seismo-stratigraphic model of Prior et al. (1986) and used geotechnical parameters derived from morpho-stratigraphic information (Fig. 4). The resulting geological-geotechnical model is shown in Fig. 5 and will be used with the slope stability package SlopeW. The origin of the profile (Fig. 5) is taken 5 km behind the actual shelf edge, and the reference datum placed at a depth of 2200 m below present sea level. Considering that the toe of the slope could be estimated from the multibeam bathymetry and from extending the stratigraphy in the escarpment to deeper waters (see Fig. 4) we consider that the base of any deltaic accumulation could not exceed the position shown in Fig. 3. Fig. 5 shows the variation in the shape of the deltaic deposit as a function of the foreslope slope angle (from 2° to 14°). An important consideration here is that if we increase to foreslope angle, while maintaining the position of the toe of the delta, the volume of the sediments involved in the slide increase sharply. Our estimates has shown that we must keep that angle below 5° if we wish to keep the total volume of the slide (i.e. including slide 1 and slide 2) close to what has been estimated for the debris (Chaytor et al., 2007). For example, taking a foreslope angle of about 3°, the deltaic deposit (unit 1 in Fig. 5) can be draped over the underlying sedimentary sequence in a way as to maintain the estimated volume of the slide. This scenario results in a position of the offlap break, at the time of sliding, less than 1 km offshore form the current shelf edge location (Fig. 5). In any case, the effect of the foreslope angle on the factor of safety is analyzed below.

Since the geometry of the failure surface can be approximated with some confidence and that it is considered to result from a slope failure, the overall factor of safety reached a value of 1 or less under conditions that are still to be evaluated through the following back analysis. The limit equilibrium analysis considers that the forces acting on a slope are in equilibrium when the resisting forces equal the gravitational forces so that the ratio of these forces, called the Factor of Safety (F), are at unity (F = 1).

The position of the failure surface is taken as a boundary condition for the computations so that all the evaluation is done considering failures on these surfaces (slide 1 and slide 2). Slope failures 1 and 2 are considered separately here, i.e. that slide 2 takes place with a new slope geometry created by the removal of sediments by slide 1. As it has been shown by Locat et al. (2003) for the Hudson Apron area to the north, instabilities which develop on such natural slopes and low-angle failure surfaces must involve triggering conditions requiring either very high excess pore pressures or significant earthquake acceleration or both. Ultimately, this must lead to a significant reduction in the shearing resistance along the failure surface. Since it has been proposed by Prior et al. (1986) that the failure could have been triggered by an excess pore pressure resulting from sediment accumulation, we included this parameter (Eq. (2)) in our analysis. In addition, observations above (see Fig. 3) related to a potential active fault in the vicinity of the slide area, and known major historical earthquakes in the Charlestown area (M = 6.9 in 1886, Bakun and Hopper 2004, Fig. 2 of ten Brink, 2009-this volume) lead us to also consider seismic acceleration as a potential trigger for the slide (Eq. (3)).

As mentioned above, a back analysis was carried out to evaluate the effect of (1) excess pore pressure, (2) prograding deltaic sediment loading (only for slide 1), and (3) seismic acceleration for slide 1 and 2. Although not shown hereafter, considering a single failure event integrating slide 1 and 2 failure planes in a step like fashion yielded similar results for initiation of instability to what is presented hereafter.

The effect of excess pore pressure and delta progradation has been simulated together and the results, for slide 1, are shown in Fig. 7 and in Fig. 8 (for k = 0.0) for slide 2. If we consider that the estimated position of the offlap break of the delta at the time of sliding was less than 1 km from the actual shelf edge, the factor of safety (F) would vary from a value of about 6.3 with no excess pore pressure to 1.5 for a pore pressure ration of about 0.8. This is very high: i.e., a pore pressure ratio of 0.8 would imply a pore water pressure of 1600 kPa at 200 m depth. For slide 2, the factor of safety values for the same pore pressure ratios are 5.6 and about 1, respectively. The lower factor of safety values for slide 2 are largely due to the fact that the lower slope left by slide 1 is steeper than for slide 1 and also that the thickness of unit 1, relative to the lower units, is proportionally larger.

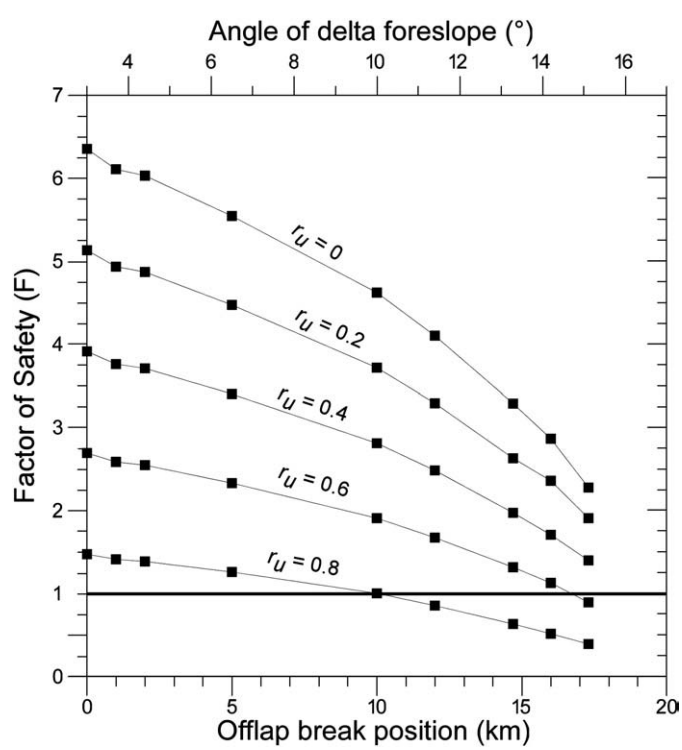

Fig. 7. Effect of excess pore pressure (r_u) and of the position of the delta edge advance on the factor of safety of the slope for slide 1 conditions.

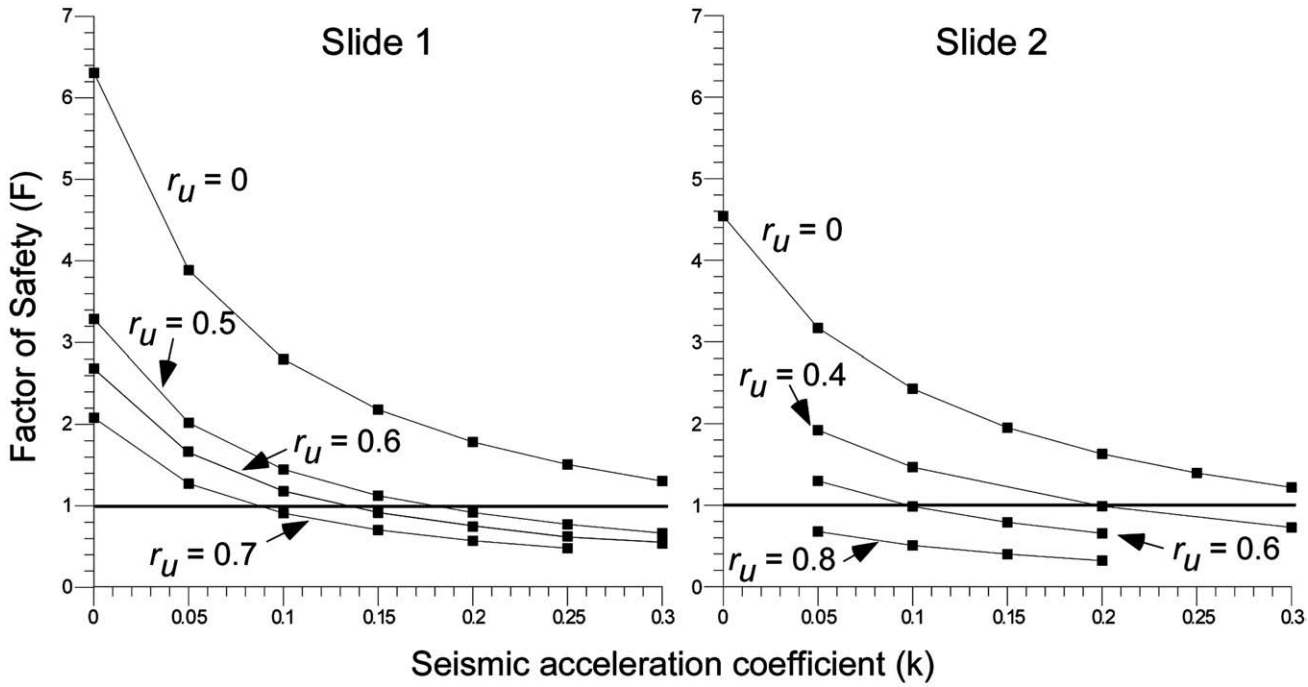

Fig. 8. Effect of earthquake acceleration on stability conditions for slide 1 and 2 as a function of the pore pressure ratio. *k* is the seismic acceleration coefficient.

The loading effect of a prograding delta (unit 1 in Fig. 5) on the underlying stratigraphic formations has been estimated by considering that the base of the slope would remain at the same location and that no excess pore pressure would be generated by the sedimentary accumulation. For example, moving the delta edge seaward 20 km increases the foreslope angle from 4° near the near shelf edge to about 14° (Fig. 5). A major consequence of moving the delta front offshore is the direct increase on the total volume of the slide up to an unrealistic level compare to the known volume. To maintain a volume similar to estimations, i.e. about 165 km^3, a realistic position of the delta edge cannot exceed 5 km seaward of the present shelf edge. Interestingly, even for a delta advancing more than 10 km (slide1 case), still significant pore pressures are required for the material to fail. The simulation in Fig. 7 suggests that the actual impact of delta advance, with the offlap break positioned at 5 km from the shelf edge, considered only as a new load, does not reduces significantly the factor of safety of the slope. It is also important to point out here that the effect of pore pressure increase, in the underlying formations, due to delta progradation, has not been considered.

To simulate the effect of seismic acceleration (earthquake loading) on the stability of the sediments, we kept a delta advance to less than 1 km (Fig. 8) so as to maintain the estimated total volume of the slide. Moving it to 5 km would reduce the overall factor of safety by about 15% (see Fig. 7). Results are shown in Fig. 8 for both slide 1 and 2. For the same reasons as indicated above, the geometry of the remaining sediments after slide takes place is such that failure of slide 2 can take place under lower excess pore pressure or seismic acceleration than slide 1. For slide 1, the analysis indicates that for moderate excess pore pressures (i.e. r_u less than 0.5), the required seismic acceleration coefficient need to be between 0.15 and 0.2 (Fig. 8). According to Fukushima and Tanaka (1990), a M6.5 earthquake located at less than 20 km could generate such acceleration while Baker et al. (2006) would propose a local M7 earthquake, This is also in accordance the work of by Keefer (1984) and Rodriguez et al. (1999) who have shown that significant mass movements can be initiated at a distance between 100 and 200 km for a M = 7 earthquake. For instability to be generated without existing excess pore pressures would require a very strong earthquake generating a seismic loading much in excess of 0.3 or an equivalent process, like water film formation (Kokusho and Kojima, 2002) that must reduce the shearing resistance to a point where it would be almost equivalent to using a r_u of zero.

In any case, the Currituck slide involved a very large volume of sediment and must have taken place under conditions likely including both existing pore pressure (or equivalent) and seismic acceleration all leading to a significant loss of strength. In the next section we will investigate the link between the run-out distance of the slide debris as a function of the volume, in the starting zone, to see weather the slide occur at once or not.

5. Mobility analysis

The preliminary geomorphological and stability analysis of the Currituck slide indicates that the slide took place under conditions that dislodged a large volume of sediment at a pace that was fast enough to almost completely clear the failure surface above the lower scarp (see Figs. 1–3). The extent of the debris generated by the Currituck slide is shown in Fig. 9 and results from the analysis of the multibeam sata and seismic surveys available in the area so that minimum volume estimates could be made (Twichell et al., 2009-this volume). The farthest distance reached by the debris was 220 km from the shelf edge and 190 km from the toe of the source area. These observations are key elements for the analysis of the mobility of the Currituck slide and provide geomorphological boundary conditions for the back analysis of the flow properties and mobility.

The bathymetry of the area inside the flow path was derived from the multibeam bathymetry, and for the purpose of modelling, we used a smoothed version of the flank profile (Fig. 10). The slope angle along this profile varies from about 8° on the upper slope to less than 0.5° on the continental rise.

5.1. Geometry

For the mobility analysis we need to define the geometry of the slide and the properties of the flowing material. BING requires a flow path, which is provided by the bathymetry (Fig. 10). The length, width, and thickness of the failing mass, at the onset of failure, are also needed. For simplicity, BING uses a half ellipse for the initial shape of the slide (see insert in Fig. 10). In our case, the shape is closer to a long

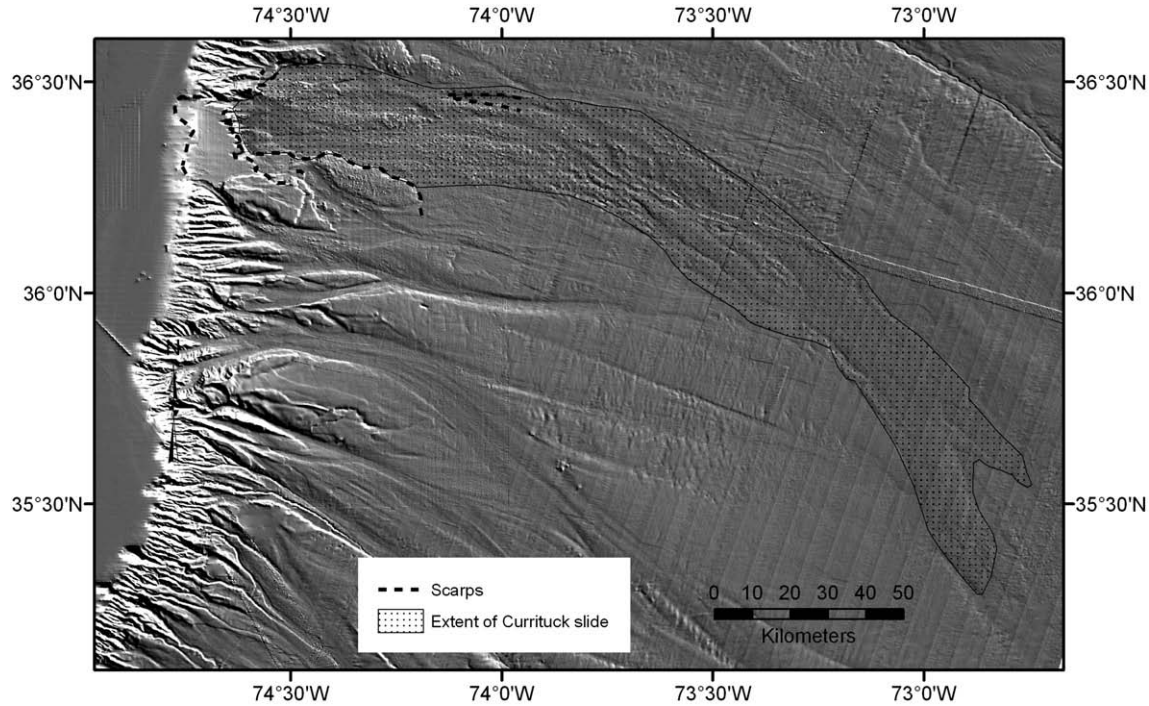

Fig. 9. Extent of the debris generated by the Currituck slide.

rectangle but, according to Imran et al. (2001a,b) it has little influence on the results. The initial geometry of the flowing mass is computed from volume estimates based on the geometry identified in Figs. 4 and 5. Here we consider that the downslope length of the failed area is about 30,000 m (30 km), and the width about 20 km. For example, if the initial thickness (H_i) in the starting zone is 250 m (see insert in Fig. 10) we get a volume of 150 km^3. If we want to simulate the volume computed by Prior et al. (1986) at 128 km^3 our estimated volume at 165 km^3, the value of H_i would be 213 m and 275 m respectively.

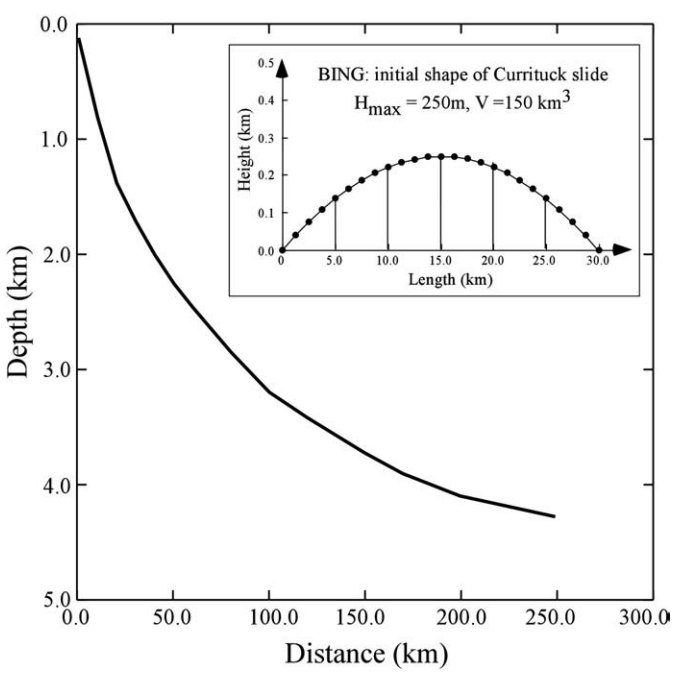

Fig. 10. Smoothed bathymetry profile used for mobility simulation using BING. Insert shows the initial shape of the flowing material use in modelling with BING (note the scale difference). The 25 nodes along the elliptical shape in the insert define the 24 elements which are individually modelled by BING. The frontal element is at a distance of 30 km from the origin.

5.2. Rheological parameters

Using Eq. (10), with a buoyant unit weight γ', of 8 kN/m^3, and β the potential slope angle at rest, and thickness (H_c) of the debris (here considered as critical since it is the final value measured in the depositional zone using seismic profiles (Twichell et al., 2009-this volume), a nomogram was computed to help select the appropriate yield strength. Results are shown in Fig. 11. Considering that the slope

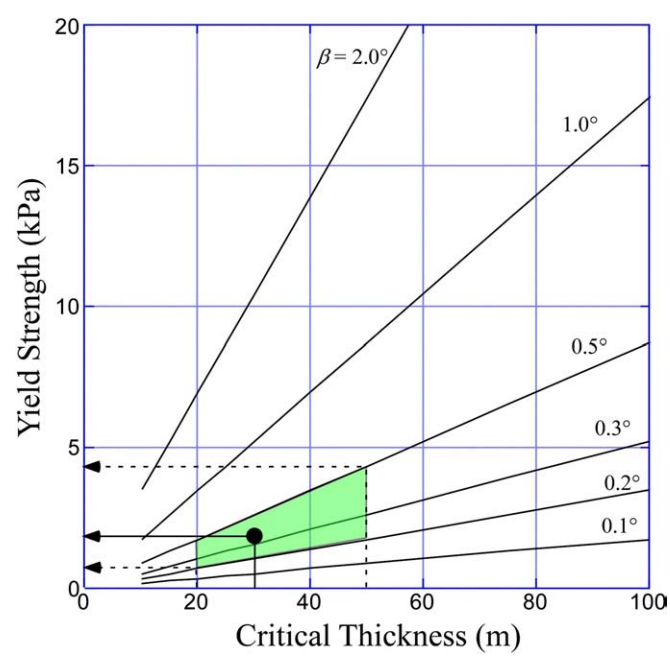

Fig. 11. Yield strength as a function of the critical height in the depositional zone. The coloured box is for a range of reported thickness for the various depositional lobes. Black dot is for a height of 30 m and a yield strength of 2.0 kPa.

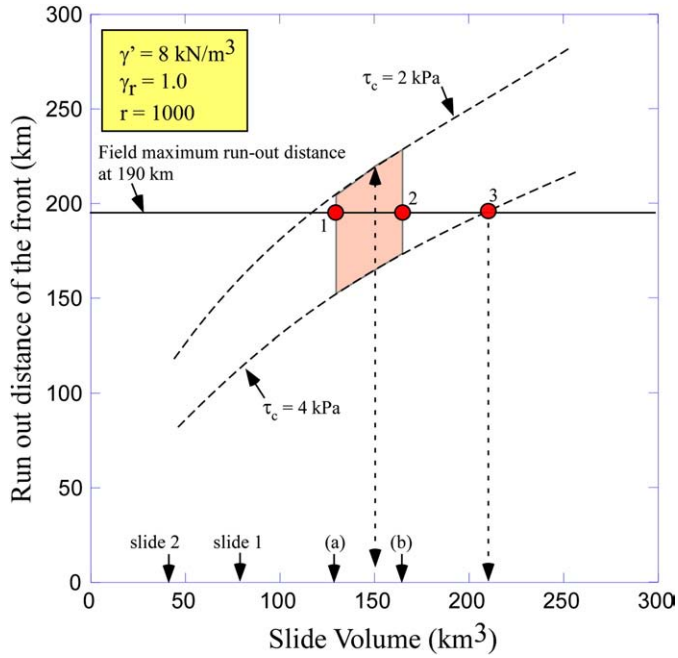

Fig. 12. Initial volume and run-out distance for two values of the yield strength. Volume at (a) is from Prior et al. (1986) and his taken at 128 km^3. Slide 1, and volume (b) is from herein computation at 165 km^3. Slide 1 and slide 2 are from models shown in Fig. 5. Field maximum run out is taken from Fig. 9. Points 1, 2 and 3 are for volumes reaching 190 km (see text for discussion).

angle in the depositional zone is between 0.2° and 0.5°, we can see that for a range in critical height (or thickness) between 20 and 50 m taken from field seismic observations of the debris (Fig. 9), the yield strength could vary more or less between 2 kPa and 4 kPa. From the yield strength, the plastic viscosity can be estimated, according to Locat (1997) and Jeong et al. (2007), to vary between 0.002 kPa s and 0.02 kPa s, i.e. has little overall influence on the fluid flow resistance.

5.3. Mobility and flow volume

Using BING with the Bilinear model the computed the relationship between the mobilized flow volume and the run-out distance of a flow over the topography and results are shown in Fig. 10. The computation was done to cover the range in yield strength, *i.e.* between 2 kPa and 4 kPa. Results are shown in Fig. 12. On that figure, we also point out four specific volumes: slide 1 and 2 of Prior et al. (1986) along with the total volume estimated by Prior et al. (1986; 'a' in Fig. 12) and our estimate ('b' in Fig. 12). On Fig. 12, we also indicate the maximum run-out distance observed from the multibeam bathymetry map of Fig. 9.

A major element to point out here is that if slide 1 and 2 are taken separately, results shown in Fig. 12 indicate that they cannot generate the observed mobility. Therefore, the various features observed in the starting zone (failure area) were created more or less at the same time indicating that, for post-failure analysis, the total volume of 150 km^3 (slide 1 + slide 2) must be used, which is close to the estimated 165 km^3 reported above. Considering that the maximum run-out distance of the frontal element cannot exceed 190 km, the analysis of Fig. 12 indicates that for the range of volume between 128 km^3 and 165 km^3 the mobilized yield strength can vary between 2 kPa and about 3 kPa. If a yield strength of 4 kPa is used, the known run-out of the debris is such that it would, for BING, require a volume of about 225 km^3, which is far too high (point 3 in Fig. 12).

From this point on, we analyse the mobility of the Currituck slide using a single volume of 150 km^3 and a yield strength of 2000 Pa.

5.4. Flow dynamics

In order to provide some insight into the tsunamigenic potential of the Currituck slide, we use BING to estimate the velocity and acceleration profile of the failing mass. It is relevant here to point out that BING, like all other flow models, assumes that the failed mass has instantaneously reached the flow properties required for the modelling, i.e. there is no transition in terms of displacements between failure and post-failure. As noted by Imran et al. (2001a,b) this will yield high initial acceleration. Still, the observed values can be used or modified according to a flow

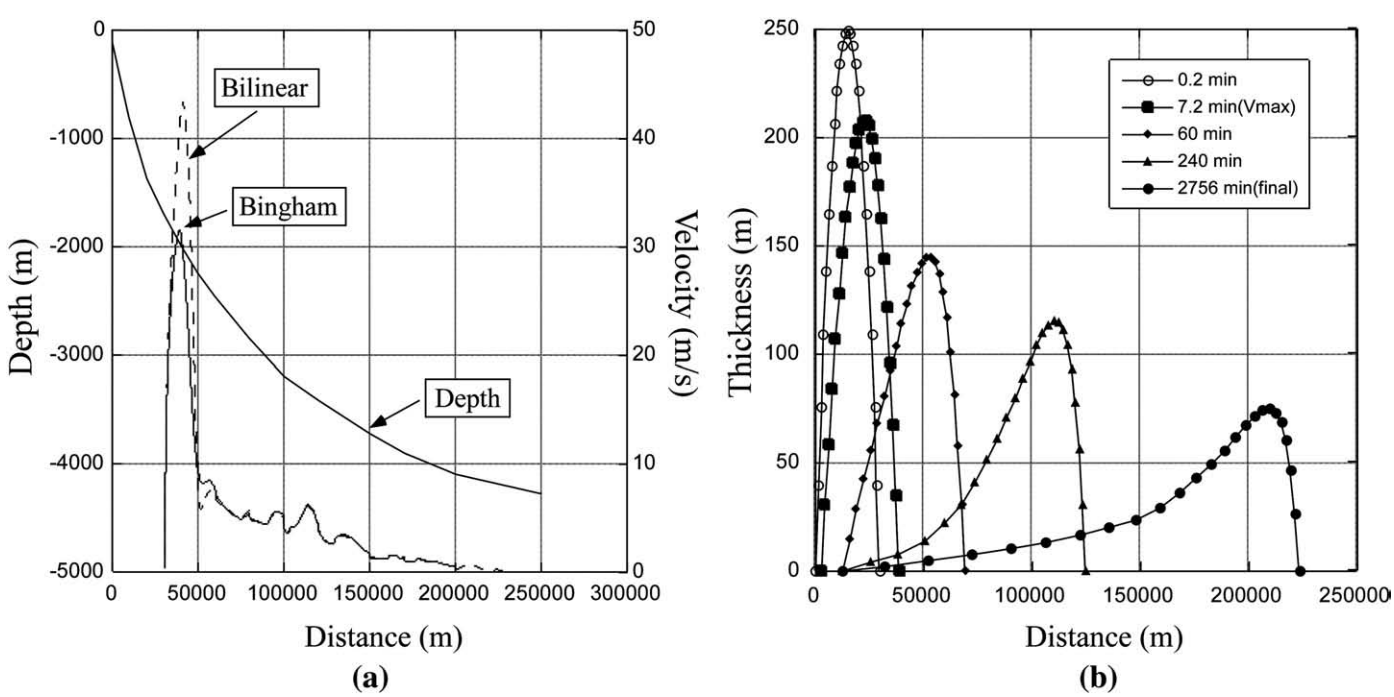

Fig. 13. Mobility analysis for Currituck slide (a) using both Bingham and Bilinear models to illustrate the velocity profile of the frontal element as a function of distance and (b) with the shape change at various time using the Bingham parameters.

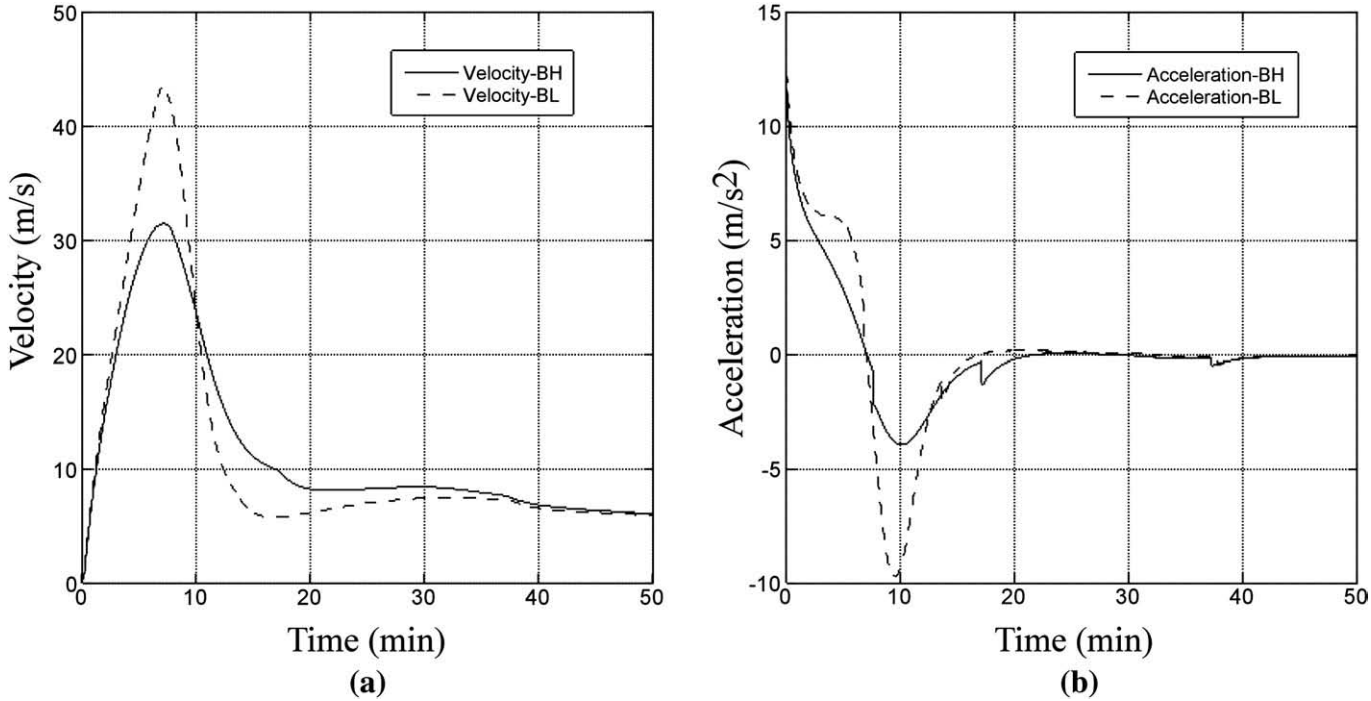

Fig. 14. (a) Velocity and (b) acceleration profile as a function of time using both Bingham and Bilinear models (BH: Bingham; BL: Bilinear).

transition model so that the initial acceleration can be adapted. For the flow dynamics, we used the two models, Bingham and Bilinear, to describe the flow behavior.

First, the velocity distribution of the frontal element, (i.e. the first one of the 24 elements subdividing the initial volume of the slide as shown in the insert of Fig. 10) as a function of distance from the toe of the slide, is shown in Fig. 13a for both Bingham and Bilinear models. As indicated by Imran et al. (2001b), the Bilinear model tends to provide higher peak velocities than the Bingham model because the Bilinear model uses a very low yield strength in the first phase of the flow. With the parameters identified above, peak velocities of 43 and 32 m/s were computed for the Bilinear and Bingham models, respectively. The stretching of the failed mass is shown in Fig. 13b for data computed using the Bingham model. The thickness varies from a maximum of 250 m, in the starting zone, to less than 50 m in the distal part for the depositional zone which is largely due to the selected value of the yield strength.

As we look at the change in velocity and acceleration with time (Fig. 14) we can see that results from both models differ in the first few minutes of the event, but otherwise are quite similar. The peak

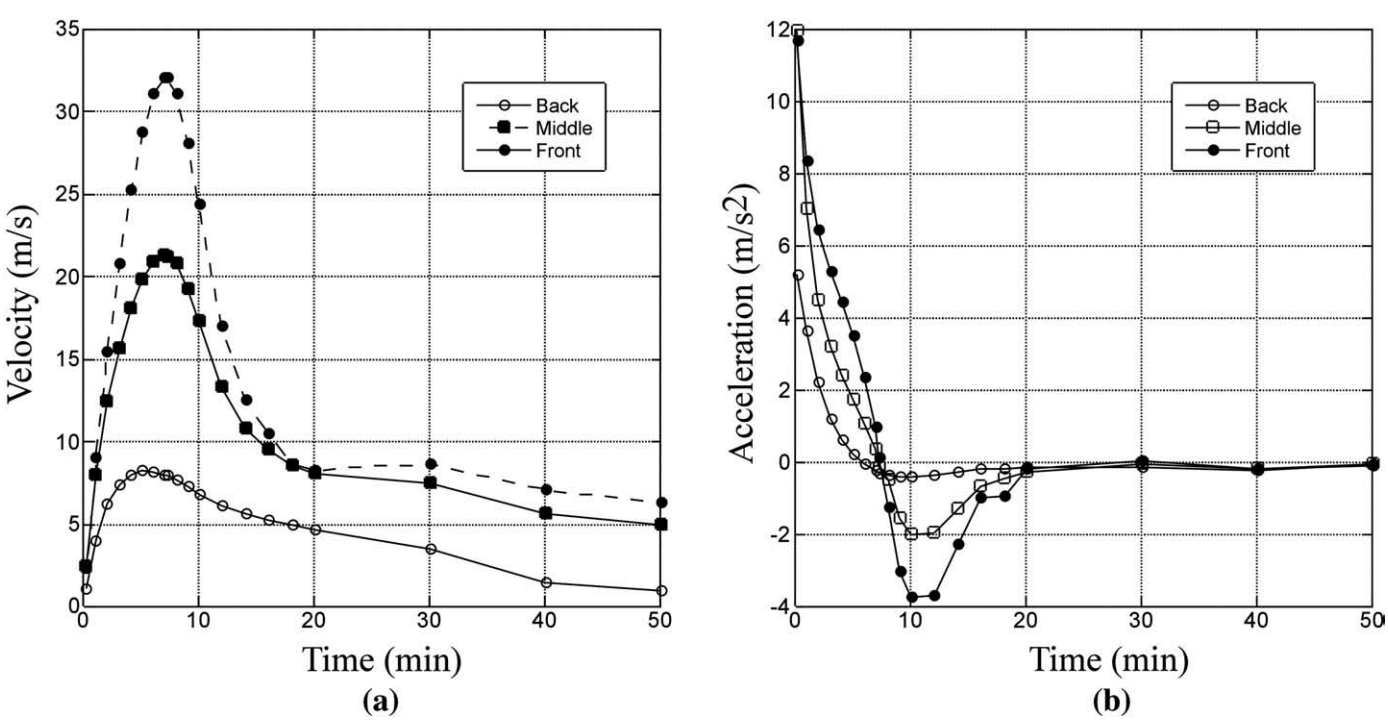

Fig. 15. (a) Velocity profiles and (b) the acceleration profiles as a function of time for the frontal, middle and back elements using Bingham model results.

velocity (or 0 acceleration) is reached at about the same time in both cases (about 7 min). Since the Bilinear model has a higher peak velocity, the deceleration is also more rapid and reaches much lower values than with the Bingham model, but the timing of the maximum deceleration is about the same in both cases, i.e. at about 10 min (Fig. 14b). After only 20 min, the deceleration proceeds very slowly until the end of the event. The initial high acceleration, expected after the above comments, is at about 12 m/s^2.

The above mobility was mostly considered for the frontal element. It is possible to extract the data to look at the behavior of a given element as is shown in Fig. 15 for frontal, middle and back elements. We can see that, for the first 10 min of the event, the absolute velocity decreases as we move away from the front (Fig. 15a). It is interesting to note that all three elements decelerate to about 0 (or reach maximum velocity) at about the same time (*i.e.* 7 min).

6. Discussion

The analysis of the stability and mobility of the Currituck slide has been carried out assuming various properties that were, in some cases, derived from field observations. The results should therefore be treated as inferences due to assumptions that had to be made as to strength parameters, pore pressure conditions, earthquake acceleration and yield strength.

6.1. Strength parameters, source of excess pore pressures, and triggering mechanism

Strength parameters were primarily derived from the known nature of the sediments involved in the slide. We feel that these are appropriate, particularly the friction angle. This is largely based on actual morphology along the upper escarpment of slide 1 and by the geometry of canyons which reveal high shearing resistance required to maintain slope angles as high as 30°. The cohesion is more difficult to establish, but considering the size of the slope, even a value of 100 kPa would have little impact on the mobilized shear strength, as it is illustrated in Fig. 6.

Choosing the appropriate pore pressure is much more difficult and can only be ascertained by *in situ* measurements that would still only provide clues on actual conditions. Our approach does, however, illustrate how much pore pressure was required to generate a failure, or its equivalent reduction in the shearing resistance of the failing mass. Our analysis also indicates that high excess pore pressures have to be developed rapidly, as it would be the case from an earthquake, to generate a failure on such low slope angles.

As we look at the morphology of the continental slope inside the Currituck slide area, it is apparent that the scarp is quite steep and high (up to 350 m, after failure). The steepness and height of the scarp indicate that the overall strength of the sediments making up this part of the slope is likely to be at least normally consolidated. In fact, if there were remaining excess pore pressure due to imcomplete consolidation of the sedimentary column, the slope angles would be much less (i.e. only few degrees). If the triggering of the Currituck slide was linked to the presence of high pore pressures generated by groundwater seepage, they clearly do not exist anymore, and if they ever existed on a more permanent basis (*e.g.* groundwater flow regime), they must have been generated after the development of strength in the sediments. In such a case, delta construction could have lead to increase pore pressures in what otherwise would have been normally consolidated sediment but the actual estimated thickness in the upper part of the slope is small in comparison to the overall geometry of the Currituck slide (Figs. 4 and 5).

Prior et al. (1986) suggested the slide took place more than 16,600 yr BP during a period of low sea level so that at that time there could have been significant changes in the groundwater flow system that may be connected to the continent. The lowering of the sea level may also have generated excess pore pressure by gas hydrates dissociation (Kayen and Lee 1991; Sultan et al., 2003) although the rate of decrease in sea level may be slow enough to prevent significant accumulation of excess pore pressure due to gas hydrate dissociation (Locat and Lee, 2009). Since the slide could have also been triggered by an earthquake, it may be possible that the local less stable conditions around the delta may be such that sliding could only take place in this part of the slope.

A compilation of earthquake epicenters along the U.S. Atlantic (Fig. 2 of ten Brink, 2009-this volume), shows that most of the epicenters are located onland. They also suggested that the Currituck slide area would fall outside of the range, for an onland earthquake of M7.5 earthquake, which could trigger a slide. The slope stability approach of ten Brink (2009-this volume) cannot include failure that would involved a rapid loss of strength, like shown by Kokusho and Kojima (2002). However, the presence of a fault-like feature on the canyon slope, just south of the slide, may support the idea that an earthquake could be the main trigger of the slide. In addition, the Charleston area, located about 600 km to the south east has experienced a M6.9 earthquake in 1886. It is interesting here to note that Bakun and Hopper (2004) indicate that the intensity center for the 1886 Charleston earthquake was located about 200 km offshore which suggests that major earthquakes could have their epicenter much closer to the continental slope than actually estimated.

From the above analysis, we are inclined to believe that the main triggering mechanism would be an earthquake but that deltaic progradation may have contributed to the development of instability.

6.2. Yield strength

For the mobility analysis, the yield strength is one of the main parameters and it can be estimated from the geomorphology of the debris in the run-out zone. A key assumption here is that we consider that the debris has been deposited all at once so that the estimated thickness of the debris in the depositional zone could be used to estimate the yield strength using Eq. (10). To that effect, more detailed seismic analysis and availability of cores (for dating post-debris flow deposit surfaces) may prove essential to validate this assumption and also confirm that the mobility could not be due to any channeling effect during the flow since this would tend to increase the run-out distance (Locat and Lee, 2005). In addition, it is not clear yet how the material can transform from a strong sediment having intact strength in the order of 100 to 1000 kPa into a fluid-like material having a much lower strength. Referring to the work of Kokusho and Kojima (2002), the generation a film of water along the failure plane, as a result of an earthquake, may provide enough remaining potential energy, after the initial failure, to be use for breaking up and remolding the sediment into a flow like material, in a way similar to what has been demonstrated for rock avalanches by Locat et al. (2006).

7. Conclusions

A review of previous work on the Currituck slide and the addition of recent multibeam surveys has provide an opportunity to re-examine this major slide along the East Coast of the United States. The analysis presented above was based mainly on morphological interpretation and on the use of typical strength characteristics of sediments.

From the above analysis we can conclude that:

1. The Currituck slide took pace as a single event.
2. It involved a volume of sediment between 150 km^3 and 165 km^3.
3. It was triggered by a catastrophic event that must have required a sudden increase in pore pressure, likely to an earthquake.
4. The mobilized yield strength was of the order of 2000 Pa.
5. The peak velocity may have been between 30 and 40 m/s.
6. Most of the acceleration phase was completed within less than 10 min.
7. The acceleration of the flowing mass is not uniformly distributed with the elements at the back having a lower acceleration than the frontal element.

Acknowledgements

This work has been made possible by the financial support of the U.S. National Regulatory Commission. The Authors would like to thank the reviewers of the Journal for their constructive comments.

Appendix A

List of symbols

c'	cohesion, kPa
c_v	coefficient of volumetric compression
E:	energy
F	factor of safety
G:	gravitational acceleration, m/s^2
H_c	critical height, m
H_i	initial thickness, m
H_f	final thickness, m
I_L	liquidity index
L_R	Run-out distance, m
k	coefficient of seismic acceleration
r	ratio of strain rates
r_u	pore pressure ratio ($u/\gamma H$)
St	sensitivity (ratio of intact to remoulded strength)
u	pore pressure, kPa
V	volume, m^3, km^3
W	Total weight of the sediment columns above the failure plane, kN

Greek symbols

α	coefficient of seismic acceleration (fraction of *g*)
β	slope angle, degree
γ	strain rate, s^{-1}
γ^*	buoyant unit weight, kN/m^3
γ_r	reference strain rate, s^{-1}
ϕ'	friction angle, degree
τ^*	shear strength, kPa
τ	flow resistance, (Pa)
τ_c	critical yield strength, Pa
τ_{ya}	yield strength considering a Bingham fluid, Pa
η	plastic viscosity, Pa s
σ	total stress, kPa

References

Baker, R., Shukka, R., Operstein, V., Frydman, S., 2006. Stability charts for pseudo-static slope stability analysis. Soil dyn. Earthqu. Eng. 26, 813–823.
Bakun, W.H., Hopper, M.G., 2004. Magnitudes and locations of the 1811–1812 New Madrid, Missouri, and the 1886 Charleston, South Carolina, earthquakes. Bull. Seismol. Soc. Am. 94, 64–75.
Barton, N.R., 1976. The shear strength of rock and rock joints. Int. J. Mech. Min. Sci. Geomech. Abstr. 13 (10), 1–24.
Booth, J.S., O'Leary, D.W., Popenoe, P., Danforth, W.W., 1993. U.S. Atlantic Continental Slope landslides: their distribution, general attributes, and implications. Submarine Landslides: Selected Studies in the U.S. Exclusive Economic Zone. U.S Geological Survey Bulletin 2002, pp. 14–22.
Bryn, P., Kvalstad, T.J., Guttormsen, T.R., Kjaernes, P.A., Lund, K.A., Nadim, F., Olsen, J., 2004. Storegga slide risk assessment. Offshore Technology Conference. Paper, vol. 16560. 14 pp.
Bunn, A.R., McGregor, B.A., 1980. Morphology of the North Carolina continental slope, Western North Atlantic, shaped by deltaic sedimentation and slumping. Mar. Geol. 37, 253–266.
Chaytor, J., ten Brink, A.R., Solow, J., Andrews, B.D., 2009. Size distribution of submarine landslides along the U.S. Atlantic Margin. Mar. Geol. 264, 16–27 (this issue).
Chaytor, J.D., Twichell, D.C., ten Brink, U.S., Buczkowski, B.J., Andrews, B.D., 2007. Revisiting submarine mass movements along the U.S. Atlantic continental margin: Implications for tsunami hazards. In: Lykousis, V., Sakellariou, D., Locat, J. (Eds.), Submarine Mass Movements and Their Consequences. Springer, Netherlands, pp. 395–403.
Christian, H., Woeller, D.J., Robertson, P.K., Courtney, R.C., 1997. Site investigations to evaluate flow liquefaction slides at Sand Heads, Fraser River delta. Can. Geotech. J. 34, 384–397.
Dugan, B., Flemings, P.B., 2005. Overpressure and fluid flow in the New Jersey continental slope: implications for failure and cold seeps. Science 289, 288–291.
Dugan, B., Flemings, P.B., Olgaard, D.L., Gooch, M.J., 2003. Consolidation, effective stress, and fluid pressure of sediments from ODP site 1073, US mid-Atlantic continental slope. Earth Planet. Sci. Lett. 215, 13–26.
Geist, E.L., Parsons, T., 2009. Assessment of source probabilities for potential tsunamis affecting the U.S. Atlantic Coast. Mar. Geol. 264, 98–108 (this volume).
Imran, J., Harff, P., Parker, G., 2001a. a numerical model of submarine debris flow with graphical user interface. Comput. Geosci. 27, 717–729.
Imran, J., Parker, G., Locat, J., Lee, H., 2001b. A 1-D numerical model of muddy subaqueous and subaerial debris flows. J. Hydraul. Eng. 127, 959–968.
Jeong, S.W., Locat, J., Leroueil, S., 2007. Rheological properties of fine-grained sediments in modelling submarine mass movements: the role of texture. In: Lykousis, et al. (Ed.), Proceedings of the 3rd International Symposium on Submarine Mass Movements and Their Consequences, Santorini. Advances in Natural Hazards Research, vol. 27. Springer, pp. 191–198.
Johnson, A.M., 1970. Physical processes in geology. Freeman Press, San Francisco.
Kayen, R.E., Lee, H.J., 1991. Pleistocene slope instability of gas hydrate-laden sediment on the Beaufort sea margin. Mar. Geotechnol. 10, 125–141.
Keefer, D.K., 1984. Landslides caused by earthquakes. Geol. Soc. Amer. Bull. 95, 406–421.
Kokusho, T., Kojima, T., 2002. Mechanism for postliquefaction water film generation in layered sand. J. Geotech. Geoenviron. Eng. 128, 129–137.
Krahn, J., 2004. Stability modeling with Slope/W: an engineering methodology. GEO-SLOPE International, Calgary, Canada. 394 pp.
Kvalstad, T.J., Andresen, L., Forsberg, C.F., Berg, K., Bryn, P., Wangen, M., 2005. The Storegga slide: evaluation of triggering sources and slide mechanics. Mar. Petrol. Geol. 22, 244–256.
Lee, H., 2009. Timing of occurrence of large submarine landslides on the Atlantic Ocean margin. Mar. Geol. 264, 53–64 (this volume).
Lee, H.J., Locat, J., Desgagnés, P., Parson, J., McAdoo, B., Orange, D., Puig, P., Wong, F., Dartnell, P., Boulanger, É., 2007. Submarine mass movements. In: Nittrouer (Ed.), Continental-margin Sedimentation: Transport to Sequence. Ch., 6.
Locat, J., 1997. Normalized rheological behaviour of fine muds and their low properties in a pseudoplastic regime. ASCE, First Conference on Debris Flows Hazards Mitigation, Mechanics, Prediction and assessment, pp. 260–269.
Locat, J., 2001. Instabilities along ocean margins: a geomorphological and geotechnical perspective. Mar. Petrol. Geol. 18, 503–512.
Locat, J., Lee, H.J., 2002. Submarine landslides: advances and challenges. Can. Geotech. J. 39, 193–212.
Locat, J., Lee, H.J., 2005. Subaqueous debris flows. Chapter 9. In: Mathias, Hungr (Eds.), Debris-flows Hazards and Related Phenomena. Springer, pp. 203–245.
Locat, J., Lee, H., 2009. Submarine mass movements and their consequences: an overview. In: Sassa, K., Canuti, P. (Eds.), Landslides – Disaster Risk Reduction. Springer-Verlag, Berlin, pp. 115–142. Heidelberg, Chapter 6.
Locat, J., Desgagnés, P., Leroueil, S., Lee, H.J., 2003. Stability of the Hudson Apron slope off New Jersey. In: Submarine mass movements and their consequences. In: Locat, J., Mienert, J. (Eds.), Kluwer series on Natural and Technological Hazards, vol. 19, pp. 257–270.
Locat, J., Lee, H.J., Locat, P., Imran, J., 2004. Numerical analysis of the mobility of the Palos Verdes debris avalanche. Mar. Geol. 203, 269–280.
Locat, P., Couture, R., Leroueil, S., Locat, J., Jaboyedoff, M., 2006. Fragmentation energy in rock avalanches. Can. Geotech. J. 43 (8), 830–851.
O'Brien, J.S., Julien, P.Y., 1988. Laboratory analysis of mudflow properties. ASCE, J. Hydraul. Eng. 114, 877–887.
Poag, C.W., Sevon, W.D., 1989. A record of Appalachian denudation in postrift Mesozoic and Cenozoic sedimentary deposits of the U.S. middle Atlantic continental margin. Geomorphology 2, 119–157.
Prior, D.P., Doyle, E.H., Neurauter, T., 1986. The Currituck Slide, Mid Atlantic continental slope-revisited. Mar. Geol. 73, 25–45.
Rodriguez, C.E., Bommer, J.J., Chandler, R.J., 1999. Earthquake-induced Landslides: 1980–1997. Soil Dyn. Earthqu. Eng. 18, 325–346.
Sultan, N., Cochonat, P., Foucher, J.P., Mienert, J., Haflidason, H., Sejrup, H.P., 2003. Effect of gas hydrates dissociation on seafloor slope stability. In: Locat, J., Mienert, J. (Eds.), Submarine Mass Movements and Their Consequences. Kluwer Advances in Natural and Technological Hazards Research, vol. 19, pp. 103–111.
Fukushima, Y., Tanaka, T., 1990. A new attenuation relation for peak horizontal acceleration of strong earthquake ground motion in Japan. Bull. Seismol. Soc. Am. 80 (4), 757–783.
ten Brink, U., 2009. Assessment of tsunami hazard to the U.S. East Coast using relationships between submarine landslides and earthquakes. Mar. Geol. 264, 65–73 (this volume).
ten Brink, U., Twichell, D., Geist, E., Chaytor, J., Locat, J., Lee, H., Buczkowski, B., Sansoucy, M., 2007. Report on the current state of knowledge regarding potential tsunami sources affecting the U.S. Atlantic and Gulf Coasts. U.S. Geological Survey Administrative Report. 164 pp.
Tinti, S., 1993. Tsunamis in the World: Fifteenth International Tsunami Symposium, 1991. Springer Publisher. 236 pp.
Twichell, D.C., Chaytor, J.B., ten Brink, U.S., Buczkowski, B., 2009. Morphology of late Quaternary Submarine Landslides along the U.S. Atlantic Continental Margin. Mar. Geol. 264, 4–15 (this volume).